Phys Chem Minerals (1997) 24: 311–317

ORIGINAL PAPER

M. T. Dove · D. A. Keen · A. C. Hannon
I. P. Swainson

Direct measurement of the Si–O bond length and orientational disorder in the high-temperature phase of cristobalite

Received August 23, 1996 /Revised, accepted January 12, 1997

Abstract Neutron total scattering measurements from powdered samples of cristobalite have been used to determine the local structure in both the tetragonal and cubic phases. The results for the cubic phase show directly that the Si–O bonds are tilted at an angle of around 17° to the unit cell [111] direction. It is striking that the structure of β-cristobalite over the range 5–10 Å is closer to that of silica glass than α-cristobalite, which suggests that the local structure of β-cristobalite is not likely to consist of domains with the structure of α-cristobalite. The measurements show a small thermal expansion of the Si–O bonds over the temperature range 570–950 K.

Introduction

The actual form of the crystal structure of the high-temperature β-phase of cristobalite has excited a lot of interest, both from direct experiment (Wright and Leadbetter 1975; Schmahl et al. 1992; Phillips et al. 1993; Swainson and Dove 1993, 1995a) and from theory (Hatch and Ghose 1991, Swainson and Dove 1995b; Hammonds et al. 1996). Standard crystal structure analyses of this phase, using the information contained in the Bragg peaks only, yielded an average structure with linear Si–O–Si bonds, and with large displacement parameters of the oxygen atoms in the directions normal to the Si–O–Si bonds (e.g. Schmahl et al. 1992). This gave average Si–O bond lengths of around 1.55 Å, which is significantly shorter than typical values (1.61–1.62 Å). One interpretation is that the oxygen atoms do not actually lie on their average positions, but instead the Si–O bonds are oriented at an angle (around 17°) to the Si...Si vector (e.g. Swainson and Dove 1995a). Thus the displacement parameters for the oxygen atoms could be interpreted as representing a distribution of oxygen positions. For example, the positions of the oxygen atoms could be disordered over an annulus, or there could be a small number of partially-occupied positions. With standard crystallography this is not an easy problem to resolve. In a typical diffraction experiment, data will be collected to a maximum value of Q ($=4\pi\sin\theta/\lambda$) of around 10 Å^{-1}. This gives a best resolution in real space, $2\pi/Q_{max}$, of only 0.6 Å, which is insufficient to pinpoint the distribution of positions with any precision. Thus so far we only have indirect evidence for the tilting of the Si–O bonds, which comes from the interpretation of the average structure deduced by diffraction (Schmahl et al. 1992; Swainson and Dove 1995a).

An alternative approach to traditional crystallographic methods is to focus on the total diffraction pattern, which includes both the Bragg peaks and the diffuse scattering. Schmahl et al. (1992) reported that there is a very strong background of diffuse scattering in the neutron powder diffraction pattern of β-cristobalite. With a time-of-flight neutron diffractometer optimised for the study of liquids and amorphous solids it is possible to obtain data for values of Q up to around 50 Å^{-1}, which in principle will give an increase in the real-space resolution by a factor of 5. Analysis of the total diffraction pattern with methods more commonly used for the study of liquids and amorphous solids should make it possible to extract quantitative information about the local structure directly.

In the present paper we report measurements of the total neutron scattering from β-cristobalite for various temperatures. We also have some data for the low-temperature α-cristobalite phase for comparison. Our objective is to determine directly the local atomic environment

Martin T. Dove (✉)
Department of Earth Sciences, University of Cambridge,
Downing Street, Cambridge, CB2 3EQ, UK
e-mail: martin@minp.esc.cam.ac.uk

David A. Keen · Alex C. Hannon
Isis facility, Rutherford Appleton Laboratory,
Chilton, Didcot, Oxfordshire, OX11 0QX, UK
e-mail: davekeen@isise.rl.ac.uk, ach@isise.rl.ac.uk

Ian P. Swainson
Neutron and Condensed Matter Science,
Atomic Energy of Canada Limited, Chalk River Laboratories,
Chalk River, Ontario, K0J 1J0, Canada
e-mail: swainsoni@cp7.aecl.ca

in order to compare with that suggested by the ideal structure. Whilst diffraction can only give information about two-particle correlations (e.g. Si–O and O–O bond lengths), rather than the three-particle correlations (e.g. O–Si–O and Si–O–Si bond angles), with reasonable assumptions it may be possible to extract average bond angles or bond orientations from the distribution of bond lengths.

Background theory for the analysis of the total diffraction pattern

The total diffraction pattern contains information about the short-range correlations through the pair distribution functions (Wright 1993, 1994). If, for a monatomic material, we define $g(r)$ such that $g(r)\mathrm{d}r$ gives the number of neighbours from a reference atom at radial distances between r and $r+\mathrm{d}r$, we can define the radial number density $\varrho(r)$:

$$g(r)\,\mathrm{d}r = 4\pi r^2 \varrho(r)\,\mathrm{d}r$$

The average number density ϱ_0 is then the spatial average of $\varrho(r)$. The most useful correlation function is

$$t(r) = 4\pi r \varrho(r) = g(r)/r$$

since this is the function that is given by Fourier transformation of the experimental data (see below). It has the properties that the experimental broadening of the peaks in the function is independent of r and symmetric. Furthermore, the experimental 'noise' in $t(r)$ is also constant across the range of r, so that ripples in $t(r)$ at low values of r, where $t(r)$ is ideally expected to be zero, give a good indication of the likely accuracy of $t(r)$ at higher values of r (Wright 1993).

In a material with more than one type of atom, we need to define the partial correlation functions $t_{ij}(r)$ for pairs of different atoms labelled i and j. If the scattering factor for a given atom is b_i (which for neutron scattering will be independent of Q), the contribution of each function $t_{ij}(r)$ will be weighted by the product $b_i b_j$. In a single experiment, where we cannot separate the different functions $t_{ij}(r)$, the data will give a measurement for the total correlation function:

$$T(r) = \sum_{i,j} b_i b_j t_{ij}(r)$$

The intensity of a radiation beam scattered from an ensemble of atoms is given as

$$\begin{aligned} I(\mathbf{Q}) &= \sum_{i,j} b_i b_j \exp\{i\mathbf{Q}\cdot(\mathbf{r}_i - \mathbf{r}_j)\} \\ &= \sum_j b_j^2 + \sum_{i\neq j} b_i b_j \exp\{i\mathbf{Q}\cdot(\mathbf{r}_i - \mathbf{r}_j)\} \end{aligned}$$

In a powder sample (as also in a glass or fluid), the diffraction measurements give the isotropic average of this quantity:

$$\begin{aligned} I(Q) &= \sum_j b_j^2 + \sum_{i\neq j} b_i b_j \frac{\sin Qr_{ij}}{Qr_{ij}} \\ &= \sum_j b_j^2 + \sum_{i\neq j} b_i b_j \int_0^\infty t_{ij}(r) \frac{\sin Qr}{Q}\,\mathrm{d}r \\ &= \sum_j b_j^2 + \int_0^\infty T(r) \frac{\sin Qr}{Q}\,\mathrm{d}r \end{aligned}$$

To obtain $T(r)$ from experimental measurements of $I(Q)$ one could, in principle, perform a reverse transform. However, there are two problems. First, it is not possible to determine the intensity of the forward scattered beam, $I(0)$. Second, measurements of $I(Q)$ are only taken to a maximum value of Q, Q_{max}. The latter problem can result in termination ripples in the Fourier transform, and is solved by multiplying $I(Q)$ in the transform by a modification function $M(Q)$ that falls smoothly to zero for values of Q greater than Q_{max}. This of course carries the cost of the broadening of the diffraction peaks. In our analysis we used the function (Lorch 1969)

$$M(Q) = Q_{max} \frac{\sin(\pi Q/Q_{max})}{\pi Q}$$

To overcome the first problem, it is common to define the interference function (Wright 1993):

$$Qi(Q) = QI(Q) - Q\left(\sum_j b_j^2 + I(0)\right)$$

The reverse transform can then be expressed as

$$T(r) = \frac{2}{\pi}\int_0^\infty Qi(Q)M(Q)\sin(Qr)\,\mathrm{d}Q + 4\pi r\varrho_0\left(\sum_j bj\right)^2$$

In principle it is necessary to take account of the resolution of the diffractometer, which is seen by the broadening of Bragg peaks. In practice, the effect of neglecting resolution is to have $T(r)$ multiplied by the Fourier transform of the resolution function, and if the resolution is reasonably good the Fourier transform will be a slow function in r that does not significantly alter the form of $T(r)$ at low r. The experimental form of $T(r)$ was extracted from the experimental data for $Qi(Q)$ using in-house software, which also gave a smooth interpolation between the points separated by $2\pi/Q_{max}$.

Experimental

The samples were prepared by annealing pure samples of silica glass at 1000 K for 6 days. Neutron and X-ray powder diffraction measurements showed that the samples had completely converted to the crystalline phase, and that there was no impurity phases present. About 3 cm^3 of powdered sample were used in the total scattering experiments, contained in a cylindrical vanadium can of 6 mm diameter. The temperature was maintained by a vacuum furnace with a cylindrical vanadium heating element.

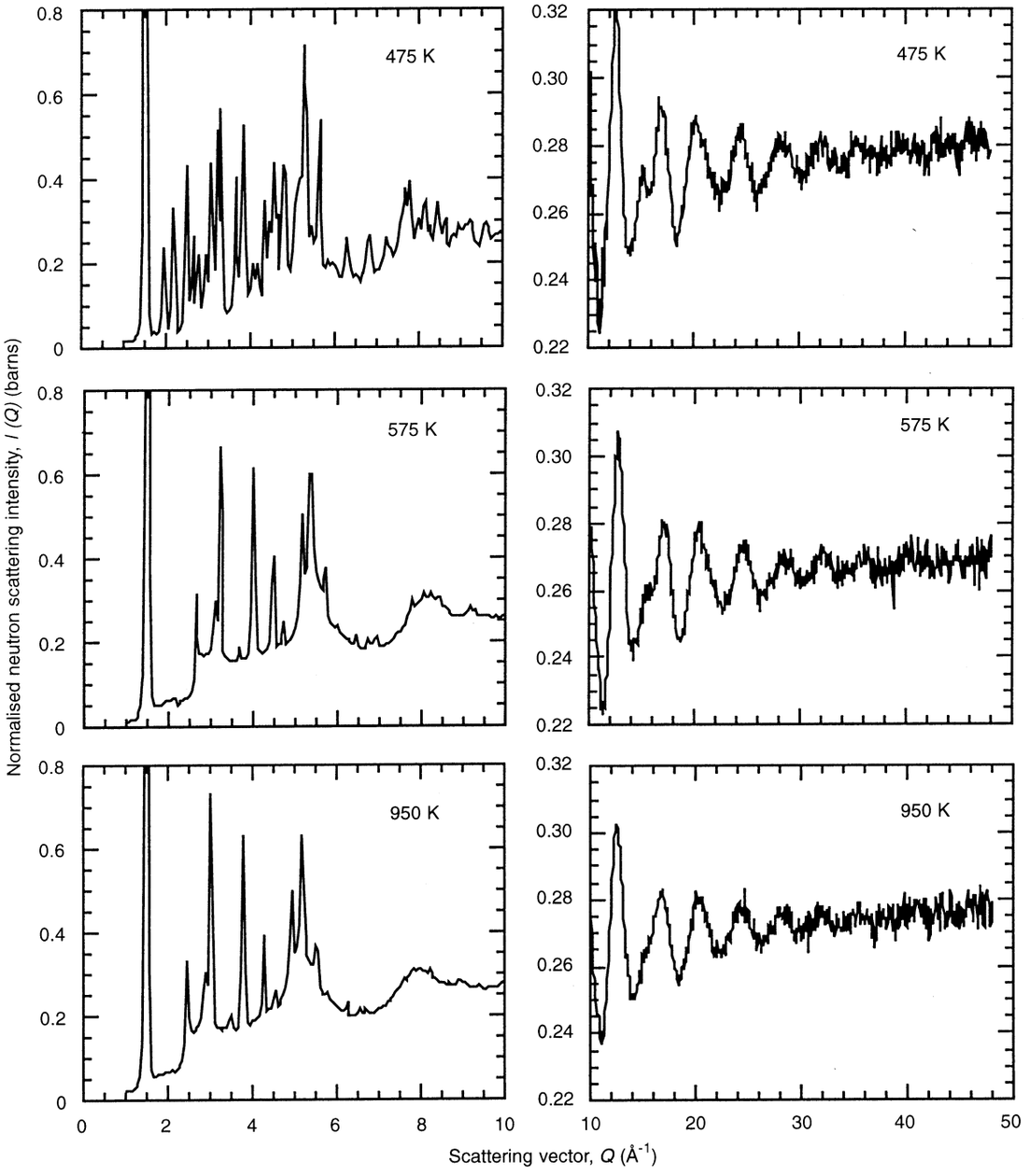

Fig. 1 Normalised neutron scattering intensity for α-cristobalite at 475 K and β-cristobalite at 575 K and 950 K, plotted over two ranges to show the Bragg peaks at low *Q* and the oscillations at high *Q*

The total neutron scattering measurements were carried out on the LAD diffractometer at the ISIS pulsed spallation neutron source. Data were collected from banks of detectors with seven distinct diffraction angles; the diffraction angles are held constant, and the data are collected by measuring the time taken for the neutrons from a single sharp pulse to travel from the target to the detectors. The flight time effectively gives the neutron wavelength, and hence, knowing the scattering angle, *Q* also. The different angles of the detector banks allow data to be collected for different ranges of *Q*: the low-angle banks collect data for lower ranges of *Q* than the higher-angle banks, and with a lower resolution in *Q*.

Data were collected for five different temperatures, each run lasting about a day. Spectra were also collected for the background with no sample or furnace in place, for the background with an empty sample can inside the furnace, and for a rod of vanadium held in the place of the sample. Each spectrum was normalised against a monitor spectrum to normalise against the wavelength distribution in the incident neutron flux.

The diffraction angles of the different detectors were calibrated against the positions of the Bragg peaks in the

diffraction pattern of β-cristobalite at 575 K, using the known unit cell parameters which had been measured with high accuracy (Swainson and Dove 1995a). The spectra from the different detectors in each bank were added together, along with the detectors for the same scattering angle at the opposite side of the sample. Corrections for the different contributions to the background signals, for absorption, and for normalisation onto an absolute scale were made to the data using standard methods (Howe et al. 1989; Hannon et al. 1990), together with the Placzek corrections (Grimley et al. 1990). The data from different banks of detectors were merged together to produce a set of single normalised structure factors, which in turn were then transformed to form $T(r)$.

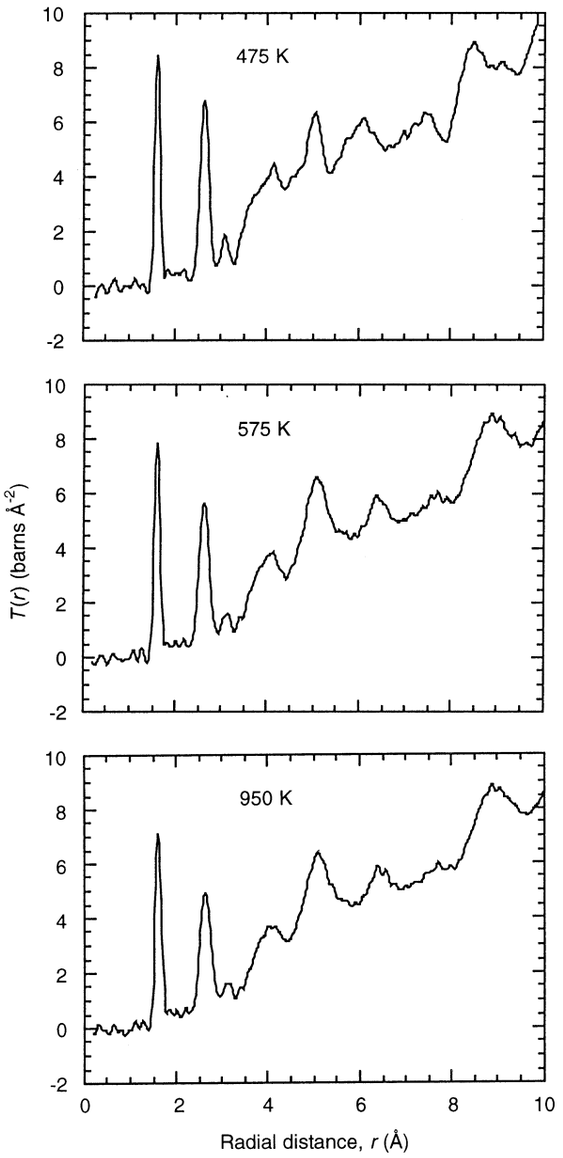

Fig. 2 Experimental correlation functions for α-cristobalite at 475 K and β-cristobalite at 575 K and 950 K

Results and discussion

The normalised neutron scattering intensities $I(Q)$ for α-cristobalite at 475 K and β-cristobalite at 575 K and 950 K are shown in Fig. 1. The derived functions $T(r)$ are shown in Fig. 2. In most of our analysis we will focus on the lower peaks in $T(r)$. The first peak at around 1.6 Å is from the Si–O bond, the second peak at around 2.63 Å corresponds to the first O–O distance that is found in the SiO_4 tetrahedron, and the small third peak at around 3.1 Å corresponds to the Si–Si distance. In the average structure of β-cristobalite, these would correspond to the distances $\sqrt{3}a/8$, $a/2\sqrt{2}$ and $\sqrt{3}a/4$, respectively. The positions of the first two peaks in $T(r)$, and the widths of these peaks, were obtained by fitting Gaussian functions, and are given in Tables 1 and 2 respectively. The Si–Si peak is too weak to be reliably analysed in this manner, and it is not well-separated from other peaks in $T(r)$. The broad peak at around 4 Å arises from the second Si–O and O–O peaks (expected at around 3.9 Å and 4.4 Å respectively), and the broad peak at around 5 Å arises from the third Si–O and O–O peaks and the second Si–Si peak (expected at around 5.3 Å, 5.1 Å and 5.1 Å respectively).

Nearest-neighbour distances

In Table 1 we compare the actual interatomic distances obtained from the positions of the peaks in $T(r)$ with those suggested by the ideal structure (using the temperature-dependence of a determined by Swainson and

Table 1 Direct measurements of the Si–O and O–O bond lengths from the correlation functions , compared with the values obtained from the ideal structure and the lattice parameters of Swainson and Dove (1995a), together with the extracted tilt angle θ

Temperature (K)	Si−O (Å)		O−O (Å)		θ (°)
	Measured	Ideal	Measured	Ideal	
475	1.6111 (2)	–	2.627 (1)	–	–
575	1.6115 (3)	1.546	2.627 (1)	2.522	16.6
700	1.6121 (5)	1.546	2.627 (1)	2.524	16.5
825	1.6130 (5)	1.546	2.628 (1)	2.525	16.5
950	1.6148 (5)	1.547	2.630 (1)	2.526	16.7

Table 2 Values of the root-mean-square fluctuations, $\langle u^2\rangle^{1/2}$, in the Si–O and O–O bond lengths, determined from the widths of the Si–O and O–O peaks in obtained by peak fitting and taking account of the broadening introduced by the modification function $M(Q)$

Temperature (K)	$\langle u^2\rangle^{1/2}$ Si−O (Å)	$\langle u^2\rangle^{1/2}$ O−O (Å)
475	0.034	0.076
575	0.035	0.081
700	0.037	0.089
825	0.041	0.094
950	0.044	0.101

Dove, 1995a). The main point to note from the data given in Table 1 is that the Si–O and O–O distances are consistently larger than the distances given by the ideal structure. On the other hand, although we cannot determine the Si–Si distance with comparable accuracy, it does not appear to be significantly different from its ideal value. The Si–O and O–O distances, however, are consistent with the values expected for an ideal SiO_4 tetrahedron, O–O $\approx \sqrt{8/3}$ Si–O. Altogether these factors suggest that the real structure of β-cristobalite consists of near-ideal SiO_4 tetrahedra that are larger than the prediction of the ideal crystal structure – indeed, of the size typically found in crystalline and amorphous silicates – and tilted by some angle away from the symmetric orientation. The tilt of the Si–O bond, θ, is readily calculated from the bond length b: $\sin\theta = \sqrt{3}a/8b$. These angles are given in Table 1. If one simply associates the angle $180° - 2\theta$ with the average Si–O–Si angle, the results point to bond angles in the range 147°, which is typical for crystalline and amorphous silicates.

It is interesting to note the temperature dependence of the Si–O bond lengths, which should yield the intrinsic thermal expansion of this bond. The data give the coefficient of expansion of the Si–O bond, $\alpha_{Si-O} = b^{-1}(\partial b/\partial T)$, obtained as $(5.0 \pm 0.6) \times 10^{-6}\ K^{-1}$. This value is substantially smaller than the value obtained for the Si–O bond in albite by Downs et al. (1992): $11.7 \times 10^{-6}\ K^{-1}$. It is not possible to give a clear reason for the difference. On one hand, it could be that the Si–O bond simply has a different expansivity in different crystalline environments. On the other hand, there may be technical reasons why different methods give different results. The method discussed in this paper is a direct method, i.e. the bond length is given directly from $T(r)$. Any errors will arise from the normalisation procedure. The lowest-r peak in $T(r)$ will arise from the largest period oscillations in $I(Q)$, and the period of these oscillations will not be influenced by the normalisation factors that modify the magnitude of $I(Q)$. The only correction that will have an effect on the period of the oscillations in $I(Q)$ will be the calibration of Q from the detector angles. Since the same calibration applied to each temperature, even if there is a slight error in the scaling of Q and hence the scaling of r, this should be divided out in the definition of α_{Si-O}. The method used to extract α_{Si-O} from crystallographic data by Downs et al. (1992) involved correcting the value of the Si–O bond length from the values of the atomic coordinates obtained from X-ray diffraction for the effects of thermal motion, the parameters of which were also obtained from X-ray diffraction. These corrections allow for the swinging motion of the Si–O bonds, which of themselves lead to an apparent contraction of the bond with increasing temperature. Indeed, the atomic coordinates by themselves suggest a value α_{Si-O} (uncorrected) $= -3.5 \times 10^{-6}\ K^{-1}$. The correction then is actually the dominant factor: α_{Si-O} (corrected) $> |\alpha_{Si-O}|$ (uncorrected). If we take the view that α_{Si-O} should not be significantly different between β-cristobalite and feldspar, and if one accepts our argument that our direct measurements

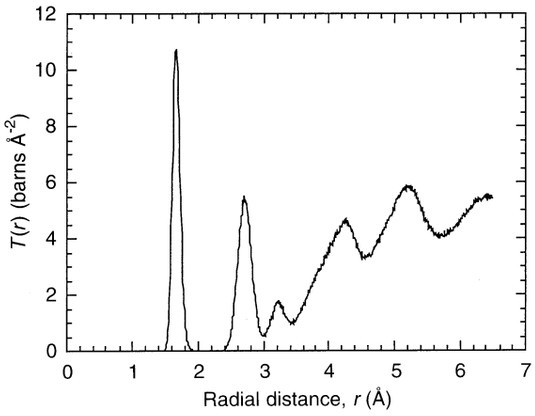

Fig. 3 Simulated correlation function for β-cristobalite at 575 K, from Swainson and Dove (1995b)

of the Si–O bond lengths lead to an accurate value for α_{Si-O}, one is left with the suggestion that the corrections of the bond length obtained by X-ray diffraction are about a factor of 2 too large. However, to counter this it should be noted that the corrected values for the Si–O bond length are between 1.604–1.627 Å (compared with the uncorrected values of between 1.595–1.602 Å), and the value we have deduced for cristobalite lies midway in the range of corrected values. We are not inclined to pursue this point any further.

The widths of the Si–O and O–O peaks in $T(r)$ increase with temperature, since they follow the root-mean-square variation in the bond length. If Γ is the full-width at half height of a peak in $T(r)$, the mean-square variation in the bond length, $\langle u^2 \rangle$, is obtained as

$$\langle u^2 \rangle = \Gamma^2 / 8 \ln 2$$

We obtained values of $\langle u^2 \rangle^{1/2}$ for the shortest Si–O and O–O bonds from the widths of their peaks in $T(r)$, taking account of the broadening introduced by the use of the modification function $M(Q)$. The results are given in Table 2. They can be fitted by the expected dependence on temperature, $\langle u^2 \rangle = \beta T$, with $\beta = (2.07 \pm 0.06) \times 10^{-6}$ Å^2 K^{-1} for the Si–O bond, and $\beta = (1.10 \pm 0.02) \times 10^{-5}$ Å^2 K^{-1} for the O–O bond. These give values for $\langle u^2 \rangle$ at 300 K that are somewhat lower than measured in silica glass (Wright 1993, 1994).

Comparison with molecular dynamics simulation

The form of $T(r)$ for β-cristobalite at 575 K was calculated from a molecular dynamics simulation by Swainson and Dove (1995b), and is shown in Fig. 3 (the function has been weighted by the appropriate neutron scattering lengths). The unit cell parameter in the simulations was 7.24396 Å (which is slightly larger than the experimental value for this temperature, 7.1328 Å, Swainson and Dove, 1992a), with the first peak in $T(r)$ giving the average Si–O bond length of 1.655 Å. In this case the Si–O

and O–O peaks are consistent with the existence of regular SiO_4 tetrahedra tilted at an angle of 18.6° from [111]. Aside from the slight differences in length scales, the calculated $T(r)$ for β-cristobalite is very similar to the measured form, although the calculated function only extends to 6 Å. The simulations showed that the Si–O bonds precess around the [111] vectors with no preferences for special sites about these axes, and these motions occur over a very short time scale. In effect, the simulations gave a dynamically disordered phase with rotations of nearly-rigid SiO_4 tetrahedra.

Comparison of $T(r)$ for the two phases of cristobalite

The form of $T(r)$ for β-cristobalite and α-cristobalite can be compared in Fig. 2. In broad terms the low-r forms of $T(r)$ are very similar. In fact, from Table 1 it can be seen that the size of the tetrahedra for both phases map directly onto the same linear function. The differences between the forms of $T(r)$ arise for values of r greater than around 5 Å, which reflects the different long-range structures of these two phases (although it could be argued that the Si–Si peak in $T(r)$ is sharper for α-cristobalite). It should be noted from Fig. 2 that the forms of $T(r)$ for β-cristobalite at 575 K and 950 K are much more similar, even though there is a much larger change in temperature than that between the spectra for α-cristobalite (475 K) and β-cristobalite at 475 K. This allows us to conclude that the medium-range order, namely over a length scale greater than 5 Å, is not the same in the two phases.

One of the models proposed to account for the tilting of the SiO_4 tetrahedra away from their ideal orientations in β-cristobalite invokes the existence of small domains of the structure of the α-phase, with the average structure of the β-phase being the average over 12 different orientations of these domains (Hatch and Ghose 1991). Although it is not possible when proposing such a model to indicate the characteristic length scale of these domains, it is essential that they should be somewhat larger than the size of the unit cell. The fact that the structures of the two phases diverge at a distance as short as 5 Å calls into question the existence of domains of the α-phase in the β-phase structure. The result from the $T(r)$ functions is more consistent with models that propose the existence of a dynamically disordered phase, one of which is the rigid unit mode model, which proposes the existence of planes of low-frequency modes that can cause rotations of the SiO_4 tetrahedra without (to lowest order) any distortions of the tetrahedra (Hammonds et al. 1996; Dove 1997). This model has been discussed in relationship to the structure of β-cristobalite in a number of previous publications (Swainson and Dove 1993, 1995b; Hammonds et al. 1996).

Comparison of $T(r)$ for cristobalite and silica glass

Finally, we also compare the form of $T(r)$ for β-cristobalite with that for silica glass (e.g. Wright 1994; Polsen et al. 1995). The functions for the distances within the SiO_4 tetrahedra are very similar, giving similar peak positions and widths. At distances greater than 6 Å, corresponding to the correlations between neighbouring tetrahedra, there is sharper structure in $T(r)$ for β-cristobalite than for silica glass, which is a reflection of the existence of the crystallographic order in β-cristobalite. Nevertheless, the forms of $T(r)$ for β-cristobalite and silica glass have more similarities for distances greater than 5 Å than the forms of $T(r)$ for β-cristobalite and α-cristobalite.

Conclusions

Our first conclusion is that the local structure of β-cristobalite, with Si–O–Si bond angles around 147°, is significantly different from the average structure with linear bonds. The local structure of β-cristobalite is fully compatible with the existence of ideal SiO_4 tetrahedra, suggesting rotations of these units. Whilst the medium-range structure of β-cristobalite is sharper than for silica glass, it is actually closer to silica glass than to α-cristobalite. We cite this result as evidence against the crystal structure of β-cristobalite containing small domains of the α-cristobalite structure.

Our second conclusion is that measurements of the total scattering provide a useful alternative route for the study of crystal structures, particularly when there is a lot of disorder. The information contained in $T(r)$ is complementary to the information contained in the average structure as given by the Bragg peaks alone. What is particularly useful about measurements of $T(r)$ is that we obtain *direct* information about local structures and fluctuations from the average structure. This information can only be deduced indirectly from analysis of the intensities of Bragg peaks, for example, using the thermal parameters to correct the apparent bond lengths. In principle total-scattering measurements can be obtained to much higher values of Q than measurements of Bragg peaks, which leads to a higher resolution in real space. In problems where the disorder involves motions over length scales just inside the 1 Å scale, measurements of $S(Q)$ to the large values of Q possible have definite advantages over measurements of Bragg scattering. An alternative to measurements of $S(Q)$ to probe local structure is the method of EXAFS, which also gives $T(r)$. However, EXAFS only gives $T(r)$ for distances out to the first shell of neighbours in a typical case, and to the second shell in special cases, and hence cannot give information about both the local and medium range order. In the present study we have compared the form of $T(r)$ for different phases to draw conclusions about changes in medium-range order when the local structures are very similar.

Acknowledgements This work was supported by provision of neutron beam time at ISIS, funded by EPSRC.

References

Dove MT (1997) Silicates and soft modes. In: Thorpe MF, Mitkova MI (ed) Amorphous Insulators and Semiconductors: Proceedings of NATO ASI. Kluwer, Dordrecht, vol 23, pp 349–383

Downs RT, Gibbs GV, Bartelmehs KL, Boisen MB (1992) Variations of bond lengths and volumes of silicate tetrahedra with temperature. Am Mineral 77: 751–757

Grimley DI, Wright AC, Sinclair RN (1990) Neutron scattering from vitreous silica. IV. Time-of-flight diffraction. J Non-Cryst Solids, 119: 49–64

Hammonds KD, Dove MT, Giddy AP, Heine V, Winkler B (1996) Rigid unit phonon modes and structural phase transitions in framework silicates. Am Mineral 81: 1057–1079

Hannon AC, Howells WS, Soper AK (1990) ATLAS: A suite of programs for the analysis of time-of-flight neutron diffraction data from liquid and amorphous samples. Institute of Physics Conference Series 107: 193–211

Hatch DM, Ghose S (1991) The α–β phase transition in cristobalite, SiO_2: Symmetry analysis, domain structure, and the dynamic nature of the β-phase. Phys Chem Minerals 17: 554–562

Howe MA, McGreevy RL, Howells WS (1989) The analysis of liquid structure data from time-of-flight neutron diffractometry. J Phys Cond Matt 1: 3433–3451

Lorch EA (1969) Neutron diffraction by germania, silica, and radiation-damaged silica glasses. J Phys C Solid State Phys 2: 229–237

Phillips BL, Thompson JG, Xiao Y, Kirkpatrick RJ (1993) Constraints on the structure and dynamics of the β-cristobalite polymorphs of SiO_2 and $AlPO_4$ from ^{31}P, ^{27}Al and ^{29}Si NMR spectroscopy from 770 K. Phys Chem Minerals 20: 341–352

Poulsen HF, Neuefeind J, Neumann HB, Schneider JR, Zeidler MD (1995) Amorphous silica studied by high-energy X-ray diffraction. J Non-Cryst Solids 188: 63–74

Schmahl WW, Swainson IP, Dove MT, Graeme-Barber A (1992) Landau free energy and order parameter behaviour of the α-β phase transition in cristobalite. Z Kristallogr 201: 125–145

Swainson IP, Dove MT (1993) Low-frequency floppy modes in β-cristobalite. Phys Rev Lett 71: 193–196

Swainson IP, Dove MT (1995a) On the thermal expansion of β-cristobalite. Phys Chem Minerals 22: 61–65

Swainson IP, Dove MT (1995b) Molecular dynamics simulation of α- and β-cristobalite. J Phys Cond Matt 7: 1771–1788

Wright AC (1993) Neutron and X-ray amorphography. In: Simmons CJ, El-Bayoumi (ed) Experimental techniques of glass science. Ceramic Transactions, American Ceramic Society, Westerville, pp 205–314

Wright AC (1994) Neutron scattering from vitreous silica. V. The structure of vitreous silica: What have we learned from 60 years of diffraction studies? J Non-Cryst Solids 179: 84–115

Wright AF, Leadbetter AJ (1975) The structures of the β-cristobalite phases of SiO_2 and $AlPO_4$. Philos Mag 31: 1391–1401